

# Dual Output Sinusoidal Oscillator Using Second Generation Current Controlled Conveyor

Syed Zahiruddin, Avireni Srinivasulu and Musala Sarada

**Abstract**—Second Generation Current Controlled Conveyor (CCCII) based tunable Dual Output Sinusoidal Oscillator (MSO) is proposed. It consists of three CCCII, a resistor and two grounded capacitors. By tuning external DC bias current, the oscillator frequency and commencement of its oscillations are controlled electronically. The proposed circuit is verified using PSPICE simulator and also on laboratory breadboard using commercially available integrated circuits Current Feedback Operational Amplifier (AD844AN) and Operational Transconductance Amplifier (LM13600) at a supply rail voltage of  $\pm 6$  V. Further its nonlinearities, sensitivities, performance characteristics are also verified. Comparison of the proposed topology with the ongoing methods are also undertaken. PSPICE simulation results are verified with a low supply voltage of  $\pm 1$  V, temperature analysis, analysis by using Monte Carlo method and finally Total Harmonic Distortion (THD) is also demonstrated.

**Keywords**—Dual Output Sinusoidal Oscillator (MSO), Current Feedback Operational Amplifier (CFOA), Operational Transconductance Amplifier (OTA) and Current mode oscillators.

*Original Research Paper*

DOI: 10.7251/ELS1923060Z

## I. INTRODUCTION

DUAL Output Sinusoidal Oscillators play an important role in many applications especially in the areas like communication systems, power electronics and measurement, instrumentation and Bio-medical fields etc. Specific applications of MSO include decoupled dynamic control of six phase two-motor drive system, vector control of single-phase to three-phase pulse width modulation converter and control schemes for five-phase induction motor drives. In literature several methods are

Manuscript received 19 August 2019. Received in revised form 08 October 2019. Accepted for publication 14 October 2019.

Syed Zahiruddin is with the Department of Electronics and Communication Engineering, Vignana's Foundation for Science, Technology and Research (Deemed to be University), Guntur-522213, Andhra Pradesh (State), INDIA (e-mail: zaheer.usk@gmail.com).

Avireni Srinivasulu, Senior Member, IEEE, was with Birla Institute of Technology, BIT-Mesra, Ranchi-835215, India. He is now with the Department of Electronics and Communication Engineering, JECRC University, Jaipur-303905, Rajasthan, INDIA. (e-mail: avireni@jecrcu.edu.in (or) avireni@bitmesra.ac.in).

Musala Sarada is with the Department of Electronics and Communication Engineering, Vignana's Foundation for Science, Technology and Research (Deemed to be University), Guntur-522213, Andhra Pradesh (State), INDIA (e-mail: sarada.marasu@gmail.com).

innovated and explained to design MSO but they are prone to encounter with the problem of utilizing more number of active and passive devices for their realization. The likely features of interest are that floating resistors seldom control the frequency, further floating capacitors however restrict the high frequency operation, and also in this case, electronic tunability may not be possible [1-3]. M.S. Ansari *et al* [4] had proposed mixed mode of three phase sinusoidal oscillator realized with Dual-X Current Conveyor (DXCCII) as an active element. Its design depends on the first order inverter low pass filter, which contains DXCCII, resistors and capacitors. It involves twelve passive components and is really a complex structure for monolithic IC fabrication besides offering the benefit of grounded passive components. S. Maheshwari and R. Verma [5], have developed several oscillator circuits and drew comparison between third order and second order sinusoidal oscillator circuits. It is observed that the third order oscillator, however, has low harmonic distortion over second order. The design is involved with four CCCII to develop three low pass filters and one gain block in feedback. It has the drawback of requiring four CCCII and four passive components. In order to obviate the above restrictions, translinear based Dual Output Sinusoidal Oscillator has been proposed.

Proposed design is entailed with the following features:

1. Single grounded external resistor is required for realization of the design.
2. Utilizes grounded capacitors that are worthwhile for IC fabrication, also the chip area is reduced effectively in comparison with floating capacitor configuration and also preferred in high frequency applications.
3. Oscillator frequency and commencement of oscillations are independent of each other and thus enhances the electronic tunability.
4. Possess low passive sensitivities [6].

The design consists of three CCCII, a resistor and two grounded capacitors only. By varying the external DC bias current, the oscillator frequency and the oscillatory condition of the proposed circuit are tuned separately.

## II. CURRENT CONVEYOR

### A. Current Mode Circuits

For the past few decades, analog designers have been trusted current-mode circuits as necessary building blocks for analog circuits design. Smith and Sedra [1] had invented the first generation current conveyor (CCI), employing bipolar junction

transistors. It has the drawback of low input impedance, which is not feasible to apply in many applications. The modified CCI, called as Second Generation Current Conveyor (CCII) was introduced by the same duo in 1970. It has high input impedance and is preferred in many applications. CCCII, a series of CCII, has the parasitic resistance at input port  $X$  which is current controlled. Thus, it has introduced the concept of Current Controlled Conveyor (CCCII) [7-10].

*B. Second Generation Current Controlled Conveyor*

Basically, CCII is the current mode active structural element. It is a mixed translinear loop that has considerable amount of intrinsic resistance  $R_B$  at the input node  $X$ . It is varied by tuning the external bias current.

The state space representation, by considering the intrinsic resistance  $R_B$  of an ideal CCCII is given below in (1).

$$\begin{bmatrix} I_Y \\ V_X \\ I_Z \end{bmatrix} = \begin{bmatrix} 0 & 0 & 0 \\ 1 & R_B & 0 \\ 0 & \pm 1 & 0 \end{bmatrix} \begin{bmatrix} V_Y \\ I_X \\ V_Z \end{bmatrix} \quad (1)$$

From (1), if the direction of current at input port  $X$  and output port  $Z$  are the same, it becomes a positive current conveyor (CCCII+). If the direction of current is opposite to each other then it is a negative current conveyor (CCCII-). At node  $X$ ,  $R_B$  denotes the input intrinsic resistance, tuned with bias current, ( $R_B = V_T / 2I_B$ ), where  $V_T \approx 26$  mV is the voltage equivalent of room temperature, and  $I_B \geq 0$  is the external bias current of the CCCII [5]. At node  $Y$ , the current  $I_Y$  is zero since the impedance at the input of node  $Y$  is infinite. So, the current applied at input node  $X$  is transformed to high impedance output node  $Z$ . Several applications have been presented by applying bias current to the CCCII [9-13]. Fig. 1 shows the symbol of CCCII.

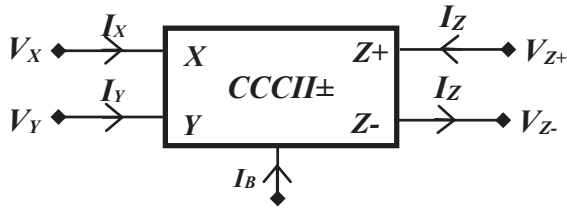


Fig. 1. Symbol of CCCII±

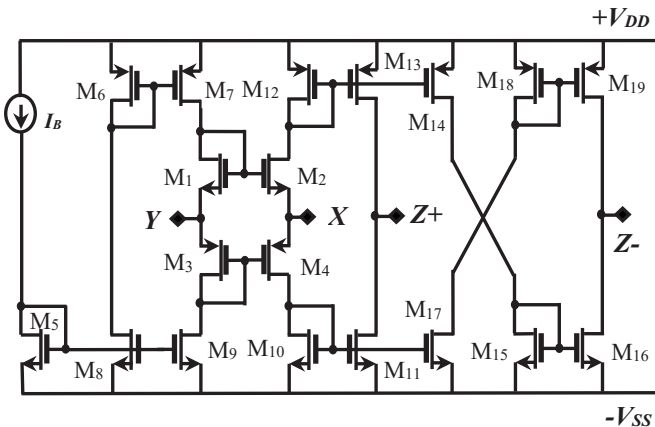


Fig. 2. Internal structure of CCCII±

CCCII is a three terminal device, two input terminals  $X$  and  $Y$  along with an output terminal  $Z$ , as shown in Fig. 2 [11]. The device is characterized by  $I_Y = 0$ ,  $V_X = V_Y + R_B I_X$  and  $I_Z = \pm I_X$ , shown in the matrix form in (1). The device has an infinite input impedance at terminal  $Y$  and  $Z$ , whereas, the input terminal  $X$  has intrinsic resistance  $R_B$  which is tuned by the external bias current  $I_B$ , given as

$$R_B = \frac{1}{g_{m2} + g_{m4}} \quad (2)$$

where  $g_{mi}$  is the transconductance of the MOS transistor, assuming that both the transistors are matched,  $g_{m2} = g_{m4}$ , then

$$R_B = \frac{1}{\sqrt{8\mu C_{OX} \left(\frac{W}{L}\right)} I_B} \quad (3)$$

where  $\mu$  is the mobility of the carrier,  $C_{OX}$  is the oxide capacitance,  $W$  is the channel width and  $L$  is the channel length of the MOS transistors ( $M_2$  and  $M_4$ ). The schematic of CCCII is realized with MOS transistors [11], as shown in Fig. 2. The circuit has translinear loop involving the transistors  $M_1$  to  $M_4$ , DC biased by using the current mirrors  $M_6$ - $M_7$  and  $M_8$ - $M_9$ . The input current  $I_X$  is duplicated to produce  $I_{Z+}$  and  $I_{Z-}$  using translinear loops. The current is replicated using additional current mirrors  $M_{10}$ - $M_{13}$ ,  $M_{14}$ - $M_{16}$  and  $M_{17}$ - $M_{19}$ . The transistor aspect ratios of Fig. 2 are shown in Table. I. For  $I_Z = +I_X$ , the device is termed as positive current conveyor and for  $I_Z = -I_X$  it is called negative current conveyor [1]. In bipolar CCCII, the intrinsic resistance  $R_B$  is inversely proportional to the bias current  $I_B$  whereas,  $R_B$  is inversely proportional to the square root of  $I_B$  for CMOS based CCCIIs.

TABLE I  
ASPECT RATIOS OF FIG. 2 TRANSISTORS

Transistor	Width ( $\mu\text{m}$ )	Length ( $\mu\text{m}$ )
$M_1, M_2$	2	0.5
$M_3, M_4$	4	0.5
$M_5, M_8, M_9, M_{10}, M_{11}, M_{15}, M_{16}, M_{17}$	5	0.5
$M_6, M_7, M_{13}, M_{14}, M_{18}, M_{19}$	15	0.5
$M_{12}$	14.2	0.5

*C. Electronically Tunable MSO using CCCII*

Figure. 3 shows the proposed electronically tunable MSO involving CCCII as an active device. Using routine analysis and current-voltage characteristics of the CCCII in (1), the characteristic equation of the proposed design is given as:

$$S^2 C_1 C_2 R_{B1} R_{eq} R_{B3} + s(C_1 R_{B1} R_{B3} - C_2 R_{eq} R_{B3}) + 2R_{B3} = 0 \quad (4)$$

where  $R_{eq} = R + R_{B2}$

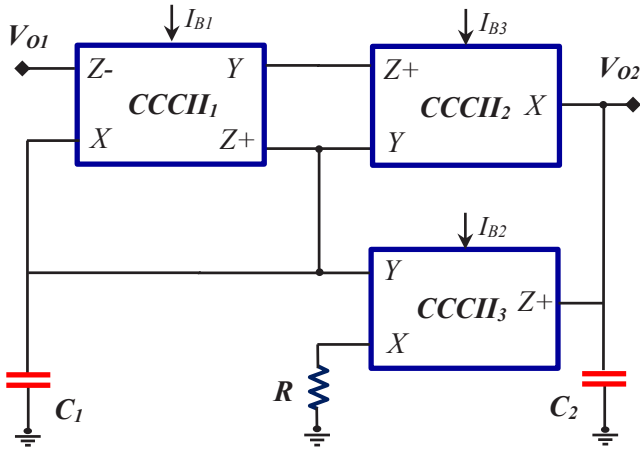


Fig. 3. Proposed electronically tunable MSO using CCCIIs

The oscillation condition and the oscillation frequency expression are realized by equating real and imaginary components of (4) to zeros and are given by

$$C_1 R_{B1} = C_2 R_{eq} \quad (5)$$

and

$$\omega = \sqrt{\frac{2}{C_1 C_2 R_{B1} R_{eq}}} \quad (6)$$

where  $R_B$  ( $R_B = R_{B1} = R_{B2} = R_{B3}$ ) refers to the parasitic resistance at the input terminals  $X$  of  $CCCII_1$ ,  $CCCII_2$  and  $CCCII_3$  due to its bias current.

Circuit as mentioned in Fig. 3 can also be inhibited to oscillate using this condition:

$$I_{B1} = I_{B2} = I_{B3} \quad (7)$$

The oscillator frequency and commencement of oscillation are controlled using bias currents.

The multiphase outputs  $V_2$  and  $V_1$  of Fig. 3, can be related as

$$\frac{V_2}{V_1} = \frac{1}{s C_1 R_{B2}} \quad (8)$$

where the phase shift is  $-90^\circ$ .

### III. NON IDEAL ANALYSIS

In practice, due to presence of non-ideal current and voltage transfer, CCCII ideal characteristics are affected that causes error to occur. Taking the non-idealities into consideration, the nodal voltages and branch currents are related as

$$\begin{bmatrix} I_Y \\ V_X \\ I_Z \end{bmatrix} = \begin{bmatrix} 0 & 0 & 0 \\ \alpha & R_B & 0 \\ 0 & \beta & 0 \end{bmatrix} \begin{bmatrix} V_Y \\ I_X \\ V_Z \end{bmatrix} \quad (9)$$

where  $\alpha = 1 - \epsilon$ ,  $|\epsilon| \ll 1$  defines the tracking error of voltage and  $\beta = 1 - \delta$ ,  $|\delta| \ll 1$  is the tracking error of current.

The characteristic equation of Fig. 3, using (9), is written as shown under

$$s^2 C_1 C_2 R_{B1} R_{eq} R_{B3} + s(C_1 R_{B1} R_{B3} - \alpha_2 \beta_2 C_2 R_{eq} R_{B3}) + 2\alpha_1 \beta_1 \beta_2 R_{B3} = 0 \quad (10)$$

Therefore, the condition for commencement of oscillation and oscillation frequency are modified respectively, as

$$C_1 R_{B1} = \alpha_2 \beta_2 R_{eq} C_2 \quad (11)$$

and

$$\omega = \sqrt{\frac{2\alpha_1 \beta_1 \beta_2}{C_1 C_2 R_{B1} R_{eq}}} \quad (12)$$

Referring to (11) and (12), the tracking errors thus slightly effect the oscillator frequency and condition of oscillation respectively. But, this effect can be minimized by improving the current gain.

According to (6) the sensitivities of passive and active components using partial derivative method with respect to the frequency are given as:

$$S_{C_1 C_2}^\omega = -1/2 \quad (13)$$

$$S_{R_B}^\omega = -1/2 \quad (14)$$

$$S_{I_{B1}, I_{B2}}^\omega = 1/2 \quad (15)$$

$$S_{V_T}^\omega = -1 \quad (16)$$

It is apparent that all parametric sensitivities of  $\omega$  are low, only 0.5 in magnitude. Thus, the design exhibits good and appealing low sensitivity value [19-21].

### IV. SIMULATION RESULTS

The proposed MSO of Fig. 3 has been simulated using PSPICE simulator. The internal schematic of CCCII was realized as shown in Fig. 2. The voltages  $\pm V_{CC} = 1V$  and the value of dc for all the CCCIIs are same,  $I_B = 100 \mu A$  ( $R_B = 260 \Omega$ ) along with  $C_1 = 8 \text{ nF}$ ,  $C_2 = 0.21 \text{ nF}$  and  $R = 10 \text{ k}\Omega$  are applied. The distinctive output simulation results of Fig. 3 is illustrated in Fig. 4, the theoretical time period is  $6.608 \mu s$ , and the simulated time period is  $5.9999 \mu s$ . The maximum oscillation frequency of  $500 \text{ kHz}$  is obtained by tuning the bias current and passive component values that are kept constant. In addition, Fig. 5 represents the simulated frequency spectrums of the output.

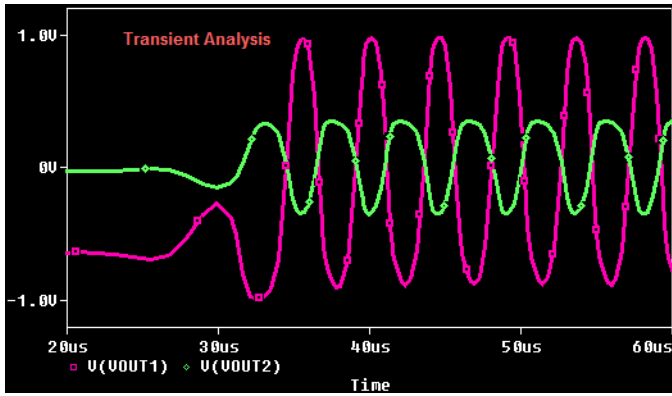


Fig. 4. The simulated output waveform of Fig.3, selected:  $I_B=100\mu A$  and  $C_1=8$  nF  $C_2=0.21$  nF and  $R=10$  k $\Omega$ .

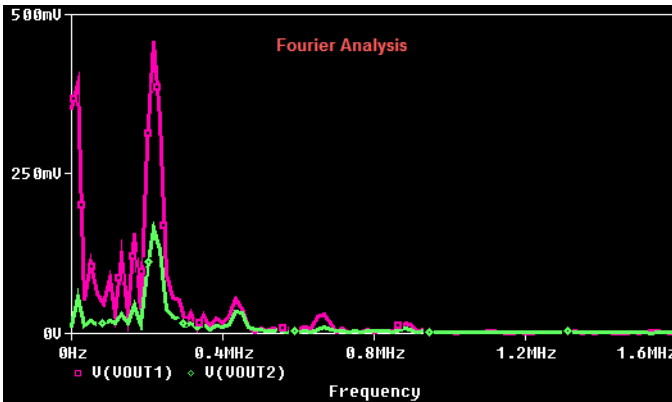


Fig. 5. Simulated output spectrums of Fig. 3, selected  $I_B=100 \mu A$  and  $C_1=8$  nF,  $C_2=0.21$  nF and  $R=10$  k $\Omega$ .

Figure 6 shows the graphic representation of variations in amplitudes of output voltages over the variation of temperature from 0° C to 100° C, keeping the bias currents and passive component values constant.

Figure 7 illustrate the simulation results of the proposed topology of Fig. 3, by varying the values of bias currents  $I_B$  (i.e.,  $I_B=I_{B1}=I_{B2}=I_{B3}$ ) versus frequency. The bias current is varied from 5  $\mu A$  to 250  $\mu A$  by maintaining  $C_1=8$  nF,  $C_2=0.21$  nF and  $R=10$  k $\Omega$  are constant. The plot specifies the linear variation of frequency with bias current, the non-idealities may be due to the ignored tracking errors.

The simulation conditions and the performance characteristics of CCCII configuration are summarized in Table II. The circuit is structured with low supply voltage of  $\pm 1$  V and has low power dissipation of the order of 1.7 mW. The total harmonic distortion is good and it is 1.97%. The input and output resistances are also measured which has exerted some influence on the performance of the circuit.

Figure 8 is the graphic representation of the Montecarlo analysis for the proposed configuration as shown in Fig. 3. The graph is produced for the 50 iterations for both the output signals. The histogram for the output signal 1 and 2 are represented in Figures 9 and 10 respectively. The mean and standard deviation values are 0.977, 0.351 and 0.0097, 0.00037 for the two signals, which are quite low and acceptable.

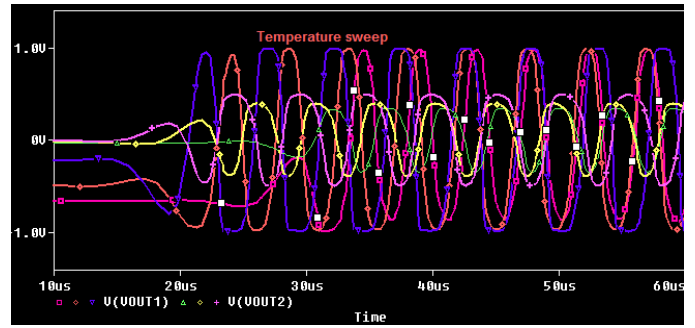


Fig. 6. Simulated results of the proposed MSO for variation in temperatures from 0° C to 100° C.

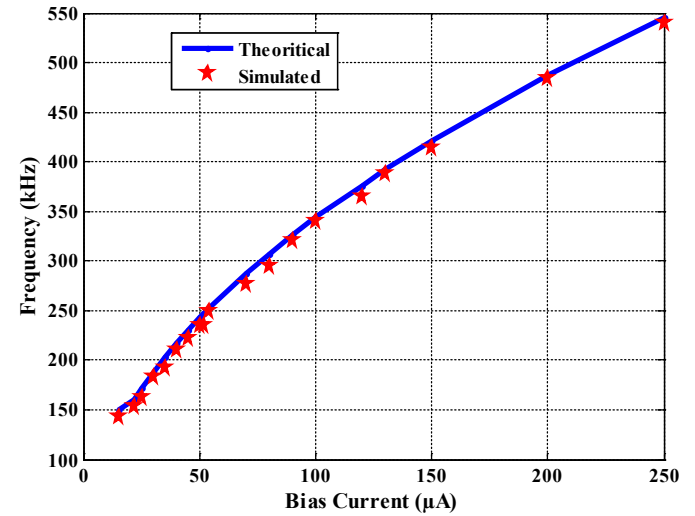


Fig.7. Simulated results of the oscillation frequency Vs bias current of Fig. 3.

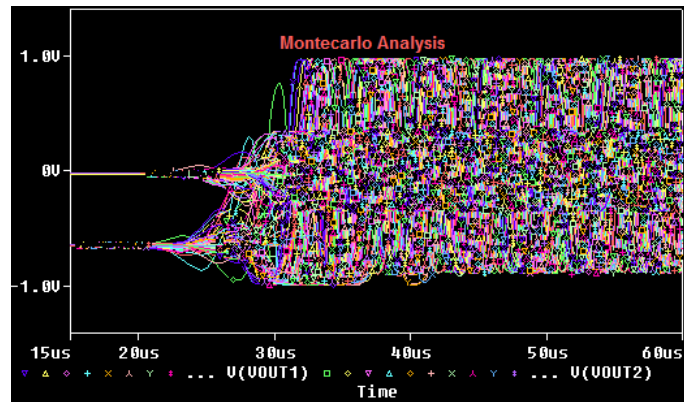


Fig. 8. Montecarlo analysis of proposed MSO

Figure 11 is the worst case analysis where as Figure 12 and 13 are the worst case sensitivities for the designed configurations. The worst case and sensitivity analysis is to identify the uncertainty in the output of a mathematical model or system. The graphs specify the insensitivity of the output and reflects the analysis as derived previously. The phase margin between the two output signals is 180 degrees and is graphically shown in Figure 14. The simulation conditions and the performance characteristics of CCCII configuration are summarized in Table

II. The input and output resistances are also measured which have exerted some influence on the performance of the circuit.

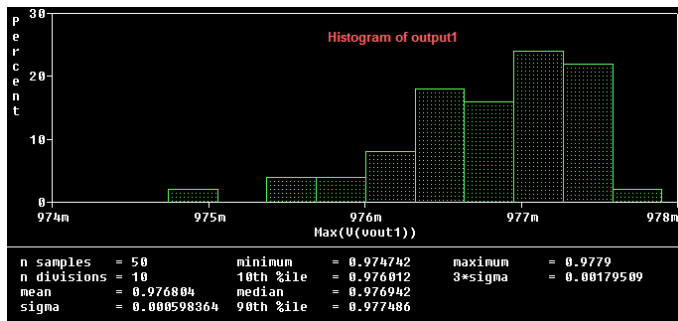


Fig. 9. Histogram for the output signal  $V_{O1}$  of the proposed MSO

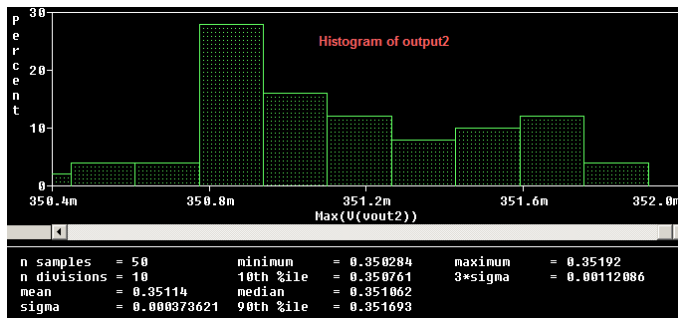


Fig. 10. Histogram for the output signal  $V_{O2}$  of the proposed MSO

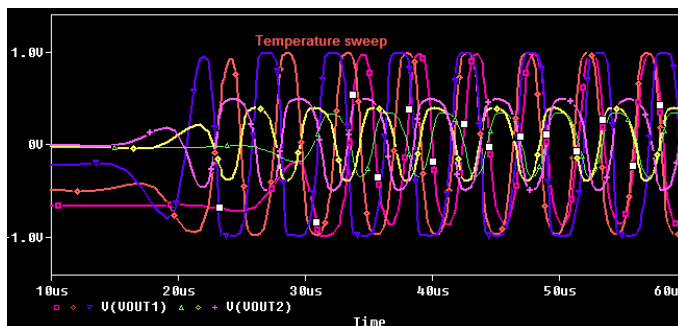


Fig. 11. Worst case analysis for the proposed MSO

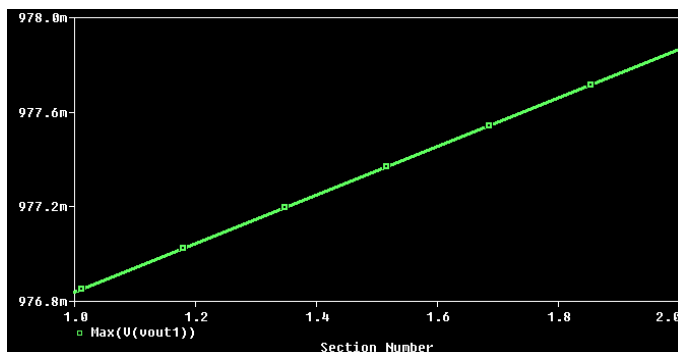


Fig. 12. Worst case sensitivity for output signal  $V_{O1}$

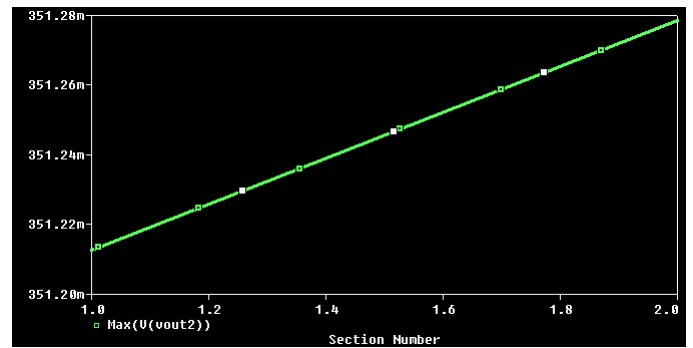


Fig. 13. Worst case sensitivity for output signal  $V_{O2}$

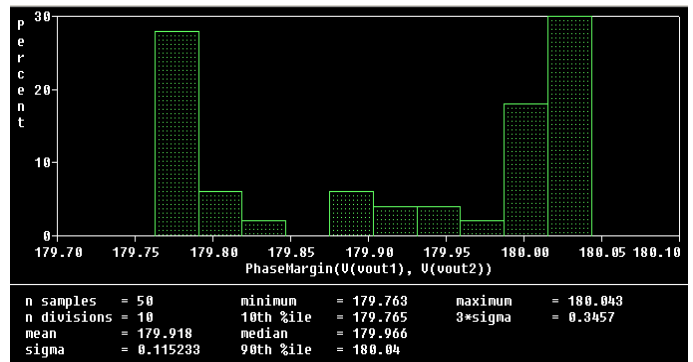


Fig. 14. Phase margin between the output signals.

TABLE II  
SIMULATION CONDITIONS AND THE PERFORMANCE CHARACTERISTICS OF CCCII

S. No	Transistor Count	PDP (aJ)
1.	Supply Voltage	$\pm 1$ V
2.	Power Dissipation	1.7065 mW
3.	Input Bias Current Linear Range	1 $\mu$ A-500 $\mu$ A
4.	$R_B$ Ranges	26 $\Omega$ to 1300 $\Omega$
5.	$R_O$	4.68 k $\Omega$
6.	$R_Z$	1.176 k $\Omega$
7.	$R_Y$	7.273 M $\Omega$
8.	Total Harmonic Distortion (THD)	1.97 %

TABLE III  
COMPARISON OF EXISTING TOPOLOGIES WITH PROPOSED MSO.

Ref	No. of active elements and type	No. of passive elements	Supply Voltage (Volts)	THD (%)	$\dagger$ PCG	$\dagger$ H/S Results
[4]	3, DXCCII	12	$\pm 1.25$	----	Yes	S
[5]	4, CCCII	4	$\pm 1.25$	2.9	Yes	S
[14]	3, ZCCDU	6	$\pm 1.5$	0.24	No	H
[15]	3, CCCII	3	$\pm 2.5$	----	Yes	S
[16]	4, CBTA	4	$\pm 1.5$	2.1	Yes	S
[17]	4, CCDU	5	$\pm 1.5$	2.2	Yes	S
This work	3, CCCII	3	$\pm 1$ ( $\pm 6$ V)	1.97	Yes	S (H)

$\dagger$ PCG: Passive Components Grounded,  $\dagger$ H: Hardware, S: Simulation



The comparative analysis of the proposed circuit is given in Table III. The proposed model employs less number of active devices and passive components for realization and are grounded. The circuits in [4] have the drawback of using more passive components. The circuit of [5] has the advantage of using less passive components but at the cost of 2.9% of the Total Harmonic Distortion (THD). The circuit in [14] has low THD of 0.24% but has the drawback that the passive components are not grounded. The grounded capacitor provides the feature such as reduced noise and low parasitic effects. The circuit of [15] has less number of active and passive devices and are grounded. Though the supply voltage as mentioned in [16] and [17] is low, but it suffers from the distortion levels of 2.1% and 2.2% respectively. While comparing the above circuits, the proposed method has the advantage of requiring less supply voltage with satisfactory THD of 1.97% and also hardware results are verified.

## V. MEASURED RESULTS

CCCI equivalent model has been put to implementation using the structure shown in Fig. 15 [18]. The hardware implementation on laboratory breadboard with external passive components of proposed MSO of Figure 3 is realized with commercially available Current Feedback Operational Amplifiers (CFOAs) of IC AD844AN [22] and Operational Transconductance Amplifiers (OTAs) of IC LM31600 [23] that produces the waveform as shown in Figure 16. For  $C_1 = C_2 = 0.01 \mu\text{F}$ ,  $I_B = 100 \mu\text{A}$ ,  $R=10 \text{ k}\Omega$  and supply voltage of  $\pm 6 \text{ V}$  are selected to produce the experimentally measured time period of  $54.79 \mu\text{s}$ , whereas, the theoretical time period is  $50.99 \mu\text{s}$  and the results are found to be close to each other. The experimental results of output voltages in  $X$ - $Y$  mode measured on oscilloscope and able to produce  $180^\circ$  phase shift as shown in Figure 17. As the tunability plot obtained for the measured results is more or less replica of the simulated ones which are already presented, and not included here.

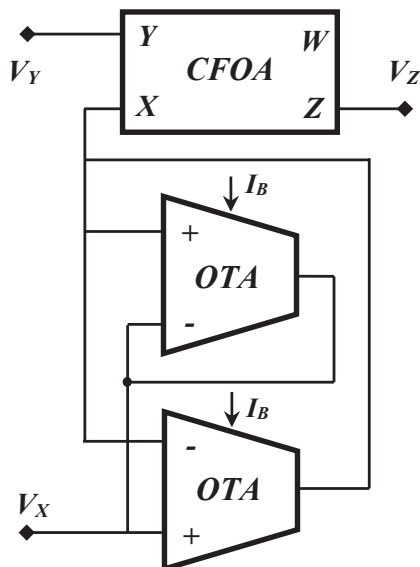


Fig. 15. Implementation of CCCII+ using CFOA and OTAs

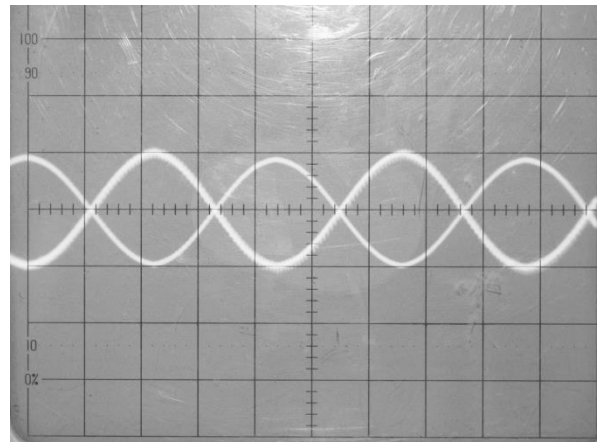


Fig. 16. Experimental results of the proposed MSO in Fig. 3. Scale X-axis:  $10 \mu\text{s}/\text{div}$  and Y-axis:  $2 \text{ V}/\text{div}$ .

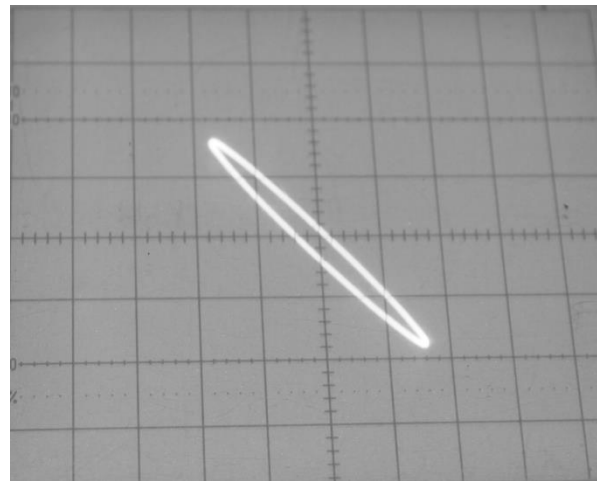


Fig. 17. Experimental results of the Fig. 3 output voltages  $V_{o1}$  Vs  $V_{o2}$ .

## VI. CONCLUSION

In this manuscript, a current mode electronically tunable Dual Output Sinusoidal Oscillator using three CCCIIIs is presented. The oscillation frequency can be tuned to a maximum of  $500 \text{ kHz}$  by tuning the external bias currents of CCCIIIs. The circuit has one resistor and two capacitors that are grounded, which is more advantageous in IC fabrication. Simulation results verifying the theoretical analysis are included along with frequency spectrums. Sensitivity parameters and performance characteristics are also determined. Hardware results of the proposed MSO are in agreement with the software results. Temperature analysis with respect to the variation of amplitudes and THD are also determined. The comparative analysis drawn for the proposed topology is made with the existing methods. The reported electronically tunable MSO has a simple structure that is requiring less area, dissipating at low power of  $1.7065 \text{ mW}$  and low THD of  $1.97\%$ .

## REFERENCES

- [1] A. S. Sedra, G. W. Roberts and F. Gohh, "The current conveyor: history, progress and new results," *IEE Proceedings (Part G) of Circuits, Devices and Systems*, vol.137, no. 2, April 1990, pp. 78-87. DOI:10.1049/jp-g-2.1990.0015.
- [2] A. Srinivasulu, "A novel current conveyor-based Schmitt trigger and its application as a relaxation oscillator," *Int. J. Circuit Theory and Applic.*, vol. 39, no. 6, pp. 679-686, 2011. DOI:10.1002/CTA.669.
- [3] A. Srinivasulu and P. Ch. Shaker, "Grounded resistance/capacitance-controlled sinusoidal oscillators using operational transresistance amplifier", *WSEAS Trans. on Circuits and Syst.*, vol. 13, pp. 145-152, 2014.
- [4] M. S. Ansari, Iqbal A Khan, Parveen Beg, Ahmed M. Nahhas, "Three passive mixed-mode CMOS VCO with grounded passive components," *Electrical and Electronics Engineering*, vol. 3, no. 6, pp. 149-155, 2013. DOI: 10.5923/j.eee.20130306.02.
- [5] S. Maheshwari, R. Verma, "Electronically tunable sinusoidal oscillator circuit," *Active and Passive Electronic Components*, vol. 2012, pp. 1-6, 2012. DOI:10.1155/2012/719376.
- [6] R. Pandey, N. Pandey, M. Bothra and S. K. Paul, "Operational Transresistance Amplifier based multiphase sinusoidal oscillators," *Journal of Electrical and Computer Engineering*, vol. 2011, pp. 1-8, 2011. DOI: 10.1155/2011/586853.
- [7] M. Kumngern and S. Junnapiya, "A sinusoidal using translinear current conveyors", in *Proc. of IEEE Asia Pacific Conference on Circuits and Systems (APCCAS)*, Kuala Lumpur, Malaysia, 06 - 09 Dec 2010, pp. 740-743, 2010. DOI: 10.1109/APCCAS.2010.5774754.
- [8] A. Bhargav, A. Srinivasulu and D. Pal, "An Operational Transconductance Amplifiers Based Sinusoidal Oscillator Using CNTFETs, in *Proc. of the 23rd IEEE International Conference on Applied Electronics*, Pilsen, Czech Republic, 11 Sept - 13 Sept, 2018, Pages-6. DOI: 10.23919/AE.2018.8501428.
- [9] S. Zahiruddin and A. Srinivasulu, "A high frequency tunable sinusoidal oscillator using single CCCII+", in *Proc. of IEEE International conference on Control, Instrumentation, Communication and Computational Technologies (ICCICCT 2015)*, pp. 490-493, 2015. DOI: 10.1109/ICCICCT.2015.7475323.
- [10] A.K.M.S. Haque, MD M. Hossain, W. Alan Davis, H. T. Russell and R. L. Carter, "Design of sinusoidal, triangular, and square wave generator using current feedback amplifier (CFOA)," *IEEE Region 5 Conference*, Kansas, USA, pp. 1-5, 2008.
- [11] P. Prommee, M. Somdunyanok, K. Angkeaw, "CCCII-based multiphase sinusoidal oscillator employing high-pass sections", in *proc. of the 6th International Conference on Electrical Engineering/ Electronics, Computer, Telecommunications and Information Technology*, Pattaya, Chonburi, Thailand, Vol. 01, pp. 530 - 533, 2009, DOI: 10.1109/ECTICON.2009.5137063.
- [12] A. Srinivasulu and D. Pal, "CCII+ Based Dual Square-Cum-Triangular Waveform Generator", in *proc. of IEEE International Conference on Electronics, Computers and Artificial Intelligence*, Targoviste, Romania, 29 June - 01 July, 2017, pp. 6. DOI:10.1109/ECAL.2017.8166422.
- [13] D. Pal, A. Srinivasulu, B. B. Pal, A. Demosthenous, and B. N. Das, "Current conveyor- based square/triangular waveform generators with improved linearity," *IEEE Tran. Instr. and Measuremen*, vol. 58, no.7, pp.2174-2180, 2009. DOI: 10.1109/TIM.2008.2006729.
- [14] Jirivavra and J. Bajer, "Current-mode multiphase sinusoidal oscillator based on current differencing units," *Analog Integrated Circuits Signal Proc.*, vol.74, pp. 121-128, 2013. DOI 10.1007/s 10470-012-9906-8.
- [15] M. Kumngern, J. Chanwutitum and K. Dejhan, "Electronically tunable multiphase sinusoidal oscillator using translinear current conveyors," *Analog Integrated Circuits Signal Processing*, vol.65, pp. 327-334, 2010. DOI: 10.1007/s 10470-010-9470-z.
- [16] M. Sabgas, U. Engin Ayten, N. Herencsar and S. Minaei, "Current and voltage mode multiphase sinusoidal oscillators using CBTAs," *Radioengineering*, vol.22, no.1, pp. 24-33, 2013.
- [17] J. Jin, L. Xiao, Xi Yang, B. Liao and S. Li, "Dual mode multiphase sinusoidal oscillator with equal amplitudes," *Engineering Review*, vol. 36, issue 3, pp. 211-220, 2016.
- [18] C. Chanapromma, N. Maneetien and M. Siripruchyanum, "A practical implementation of the CC - CFA based on commercially available ICs and its applications", in *Proc. of Int. Conf. on Electrical Engineering/ Electronics, Computer, Telecommunications and Information Technology (ECTI-CON 2009)*, Pattaya, Chonburi, 6-9 May, 2009, pp. 564-567.
- [19] M. T. Abuelma'atti and M. A. Al-Qahtani, "A new current controlled Multiphase sinusoidal oscillator using translinear current conveyors," *IEEE Transactions on circuits and systems-II, Analog and Digital processing*, vol. 45, no.7, pp. 881-885, July 1998.
- [20] A.Lahiri, "Deriving (MO) (I) CCCII based second-order sinusoidal oscillators with non-interactive tuning laws using state variable method," *Radioengineering*, vol. 20, no.1, pp. 349-353, 2011.
- [21] T. Piyatat, W. Tangsrirat and W. Surakamponorn, "Electronically tunable quadrature oscillator using current controlled voltage conveyors," in *Proc. of IEEE Conference on Electron Devices and Solid State Circuits*, pp. 133-136, Hong Kong, China, 2005. DOI: 10.1109/EDSSC.2005.1635224.
- [22] AD844 Current Feedback Op-Amp Data Sheet, Analog Devices Inc., Norwood, MA, 1990 [Online]. Available: <https://www.analog.com/media/en/technical-documentation/data-sheets/AD844.pdf> [Accessed: October 14th, 2019].
- [23] LM13600, Dual Operational Transconductance Amplifiers Data Sheet, National Semiconductor, 1995 [Online]. Available: [http://www.datasheetcatalog.com/datasheets\\_pdf/L/M/1/3/LM13600.shtml](http://www.datasheetcatalog.com/datasheets_pdf/L/M/1/3/LM13600.shtml) [Accessed: October 14th, 2019]